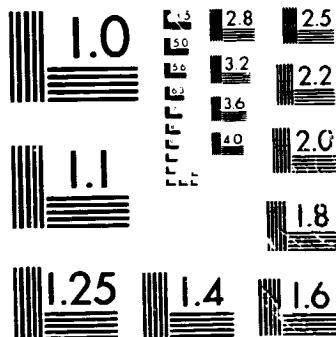


1 OF 1

N 79 27532 UNCLAS



MICROCOPY RESOLUTION TEST CHART
NATIONAL BUREAU OF STANDARDS-1963-A

NASA Technical Memorandum 80073

(NASA-TM-80073) STRESS-INTENSITY FACTORS
FOR INTERNAL SURFACE CRACKS IN CYLINDRICAL
PRESSURE VESSELS (NASA) 11 p HC A02/MF A01
CSCL 20K

N79-27532

Unclas
G3/39 29304

STRESS-INTENSITY FACTORS FOR INTERNAL SURFACE CRACKS IN CYLINDRICAL PRESSURE VESSELS

J. C. Newman, Jr., and I. S. Raju

JULY 1979



National Aeronautics and
Space Administration

Langley Research Center
Hampton, Virginia 23665



STRESS-INTENSITY FACTORS FOR INTERNAL SURFACE
CRACKS IN CYLINDRICAL PRESSURE VESSELS

J. C. Newman, Jr.
NASA Langley Research Center
Hampton, Virginia 23665

and

I. S. Raju
Joint Institute for Advancement of Flight Sciences
George Washington University at Langley Research Center
Hampton, Virginia 23665

SUMMARY

Failures of many pressure vessels have been traced to surface cracks. Accurate stress analyses of these surface-cracked components are needed for reliable prediction of their crack-growth rates and fracture strengths. Because of the complexities of such problems, all investigators have used engineering estimates or approximate analytical methods to obtain the stress-intensity factors.

A few three-dimensional stress analyses of semi-elliptical surface cracks in pressurized cylinders have been reported recently. However, these investigators considered only an internal surface crack with a crack-depth-to-crack-length ratio of $1/3$ and a wall-thickness-to-vessel-radius ratio of 0.1 .

The purpose of this paper is to present stress-intensity factors for a wide range of semi-elliptical surface cracks on the inside of pressurized cylinders. The ratio of crack depth to crack length ranged from 0.2 to 1 ; the ratio of crack depth to wall thickness ranged from 0.2 to 0.8 ; and the ratio of wall thickness to vessel radius was 0.1 or 0.25 . The stress-intensity factors were calculated by a three-dimensional finite-element method. The finite-element models employed singularity elements along the crack front and linear-strain elements elsewhere. The models had about 6500 degrees of freedom. The stress-intensity factors were evaluated from a nodal-force method. In this method, the nodal forces normal to the crack plane and ahead of the crack front were used to obtain the stress-intensity factors.

An empirical equation for the stress-intensity factors was fitted to the results of the present analysis as a function of crack depth, crack length, wall thickness, and vessel radius. The equation applies over a wide range of configuration parameters and was within about 5 percent of the present results.

The present results were compared to other analyses of internal surface cracks in cylinders. The surface-crack configuration had a crack-depth-to-crack-length ratio of $1/3$ and a wall-thickness-to-vessel-radius ratio of 0.1 . Results from the literature using a boundary-integral equation method were in good agreement (± 2 percent) and those from a finite-element method were in fair agreement (± 8 percent) with the present results.

The stress-intensity factors and equations presented herein should be useful in correlating fatigue-crack-growth rates and in calculating fracture toughness for the surface crack in a pressurized cylinder.

1. Introduction

Failures of many pressure vessels have been traced to surface cracks. Accurate stress analyses of these surface-cracked components are needed for reliable prediction of their crack-growth rates and fracture strengths. Because of the complexities of such problems, all investigators have used engineering estimates or approximate analytical methods to obtain the stress-intensity factors.

Some engineering estimates for the stress-intensity factors for surface cracks in pressurized cylinders have been made by Underwood [1] and Kobayashi [2]. Their estimates did not include the effects of wall thickness. Recently, however, Kobayashi, Emery, Polvanich, and Love [3] have estimated stress-intensity factors for internal surface cracks that did include the effects of wall thickness.

A few three-dimensional stress analyses of semi-elliptical surface cracks in pressurized cylinders have been reported recently. Atluri and Kathiresan [4] and McGowan and Raymund [5] used three-dimensional finite-element methods, while Heliot, Labbens, and Pellissier-Tanon [6] used the boundary-integral equation method, to obtain stress-intensity factor variations along the crack front for a limited range of configuration parameters. References [5] and [6] considered only an internal surface crack with a crack-depth-to-crack-length ratio of $1/3$ and a wall-thickness-to-vessel-radius ratio of 0.1.

The purpose of this paper is to present Mode I stress-intensity factors, calculated by a three-dimensional finite-element method [7-9], for a wide range of semi-elliptical surface cracks in pressurized cylinders. The cracks were located on the inside of the cylinders. The ratio of crack depth to wall thickness ranged from 0.2 to 0.8; the ratio of crack depth to crack length ranged from 0.2 to 1; and the ratio of wall thickness to vessel radius was 0.1 or 0.25. The stress-intensity factors were calculated by using a nodal-force method [7-9]. An equation for the stress-intensity factors was also developed for a wide range of configuration parameters. The stress-intensity factor variations along the crack front are presented and, where possible, compared with other solutions from the literature.

2. Symbols

a	depth of surface crack
b	half-length of pressurized cylinder
c	half-length of surface crack
f_c	ratio of boundary-correction factors (cylinder to flat plate)
F	boundary-correction factor for an internal surface crack
G_j, H_j	boundary-correction factors for j^{th} stress distribution on crack
K_I	stress-intensity factor (Mode I)
p	internal pressure on the cylinder
Q	shape factor for an elliptical crack
R, R_o	inner and outer radii of cylinder
t	cylinder wall thickness
x, y, z	local Cartesian coordinates centered at crack mouth

- X,Y,Z global Cartesian coordinates
 θ angular measurement on cylinder
 σ_j applied stress on crack surfaces
 ϕ parametric angle of elliptical crack

3. Three-Dimensional Analysis

A surface crack in an internally pressurized cylinder is shown in figure 1. The elastic cylinder of wall thickness t , internal radius R , and length $2b$, contains a semi-elliptical surface crack of length $2c$ and depth a on the inner surface of the cylinder. The stress-intensity factors for the surface-crack configurations were obtained by using a three-dimensional finite-element analysis.

3.1 Finite-Element Idealization

Two types of elements (isoparametric and singular [7]) were used in combination to model the cylindrical vessels. Figure 2(a) shows a typical finite-element model for an internal surface crack. The model, which employed nearly 6500 degrees of freedom, idealized one-eighth of the vessel ($0 \leq \theta \leq 90$ degrees and $0 \leq X \leq b$). The isoparametric (linear-strain, eight-noded hexahedron) elements were used everywhere except near the crack front, where eight singularity elements, each in the shape of a pentahedron, were used [8]. The singularity elements produced a square-root singularity in stress and strain at the crack front. A typical finite-element pattern along the crack plane is shown in figure 2(b). The finite-element models in the neighborhood of the crack were identical to those used in references [8] and [9] for surface cracks in flat plates, except that the models were curved to conform to the desired cylindrical shape. The vessel half-length-to-radius ratio, b/R , ranged from 1 to 5, the b/c ratio ranged from 10 to 50, and the t/R ratio was 0.1 or 0.25. Further details on modeling and formulation of the two types of elements used are given in references [7-9] and are not repeated here.

3.2 Boundary Conditions and Applied Loading

Symmetry boundary conditions were applied on the $X = 0$ plane, $Y = 0$ plane, and $Z = 0$ plane, and the model simulated a vessel with two symmetric surface cracks (180 degrees apart). The $X = b$ plane was free.

The stress-intensity factor solutions were obtained by solving the complementary problem of applied stresses on the crack surfaces. Four applied stress distributions on the crack surfaces were analyzed: constant, linear, quadratic, and cubic. These stresses, which were applied to the crack surfaces as shown in figure 2(c), were symmetric about the $y = 0$ plane and were given by

$$\sigma_j = \left(\frac{z}{a}\right)^j \quad \text{for } j = 0 \text{ to } 3 \quad (1)$$

where z is measured from the crack mouth toward the crack front. Solutions for these four stress distributions were superimposed to obtain stress-intensity factors for the pressurized cylinder. (These four solutions can be superimposed to obtain stress-intensity factors for other stress distributions, such as those caused by thermal shock.)

4. Stress-Intensity Factor

The Mode I stress-intensity factor, K_I , at any point along the surface crack was taken to be

$$K_I = \sqrt{\pi \frac{a}{Q}} G_j \left(\frac{a}{c}, \frac{a}{t}, \frac{R}{t}, \phi \right) \quad (2)$$

for $j = 0$ to 3 . G_j is the boundary-correction factor corresponding to the j^{th} stress distribution from eq. (1). Q , the shape factor for an elliptical crack, is given by the square of the complete elliptic integral of the second kind. The vessel length ($2b$) was always chosen large enough that the length would have a negligible effect on stress intensity ($b/c \geq 10$).

The stress-intensity factors for a surface crack in an internally pressurized cylinder were obtained by appropriate superposition of the results given by eq. (2). For convenience, the stress-intensity factor was written as

$$K_I = \frac{pR}{t} \sqrt{\pi \frac{a}{Q}} F \left(\frac{a}{c}, \frac{a}{t}, \frac{R}{t}, \phi \right) \quad (3)$$

where pR/t is the hoop stress and F is the boundary-correction factor for a surface crack on the inside of an internally pressurized cylinder. The expression for F , in terms of G_j , was obtained from the first four terms of a power-series expansion of Lamé's solution [10] for the hoop stress in an internally pressurized cylinder. The result is

$$F = \frac{t}{R} \left(\frac{R_o^2}{R_o^2 - R^2} \right) \left[2G_0 - 2\left(\frac{a}{R}\right)G_1 + 3\left(\frac{a}{R}\right)^2 G_2 - 4\left(\frac{a}{R}\right)^3 G_3 \right] \quad (4)$$

where each G_j was obtained from the appropriate finite-element solution. The correction factor F includes also the influence of the internal pressure, p , acting on the crack surfaces. Values for F were calculated as a function of a/c , a/t , and ϕ for t/R values of 0.1 and 0.25. The a/c ratios were 0.2, 0.4, and 1; and the a/t ratios were 0.2, 0.5, and 0.8.

The stress-intensity factors from the finite-element models were obtained by using a nodal-force method, details of which are given in references [7] and [9]. In this method, the nodal forces normal to the crack plane and ahead of the crack front are used to evaluate the stress-intensity factors.

5. Results and Discussion

In the following sections, results are presented for two symmetric semi-elliptical surface cracks on the inside of pressurized cylinders. The stress-intensity factor variations along the crack front for various surface cracks ($a/c = 0.2$ and 1) are presented as a function of a/t . An empirical equation for the stress-intensity factor is also developed for a wide range of configuration parameters. An estimate for the stress-intensity factor for a single surface crack is also presented. The stress-intensity factors are compared with other solutions from the literature.

5.1 Semi-Circular Surface Cracks

Figure 3 shows the boundary-correction factors for two symmetric semi-circular surface cracks ($a/c = 1$) as a function of the parametric angle, ϕ , and a/t for $t/R = 0, 0.1$, and 0.25 . For $t/R = 0$ (flat plate [8,9]), the pR/t stress in eq. (3) is replaced by S_t , a

remote uniform applied stress. For a fixed t/R ratio, the correction factors are higher for larger a/t ratios. Also, for a fixed a/t ratio, the correction factors are higher for smaller t/R ratios. The maximum correction factor (or stress-intensity factor) occurred at the intersection of the crack front with the inner surface ($\phi = 0$).

5.2 Semi-Elliptical Surface Cracks

Figure 4 shows the boundary-correction factors for two symmetric semi-elliptical surface cracks ($a/c = 0.2$) as a function of ϕ and a/t , for $t/R = 0, 0.1$, and 0.25 . Again, for a fixed t/R ratio, the correction factors are higher for larger a/t ratios. For a given a/t ratio, smaller t/R ratios gave higher correction factors. In contrast to results for a semi-circular surface crack, the maximum correction factor (or stress-intensity factor) occurred at the maximum depth point ($\phi = \pi/2$).

5.3 Stress-Intensity Factor Equation

The results shown in figures 3 and 4 suggest that the ratio of the correction factors for a given t/R and those for a flat plate ($t/R = 0$) are nearly independent of the parametric angle, so that the curve for $t/R = 0$ can be scaled to approximate the results for $t/R = 0.1$ and 0.25 . Figure 5 shows f_c (the ratio of F for a given t/R to F_0) as a function of t/R . F_0 is the correction factor for a flat plate [8,9]. The abscissas (and bars) give the average (and range) of f_c for a given value of a/t with $a/c = 0.2, 0.4$, or 1 and any value of ϕ . (For clarity, results for $a/t = 0.5$ are not shown.) These results were found to be closely approximated by

$$f_c = \left[\frac{R_o^2 + R^2}{R_o^2 - R^2} + 1 - 0.5 \sqrt{\frac{a}{t}} \right] \frac{t}{R} \quad (5)$$

In figure 5, the upper curve shows the exact limiting solution for $a/c = 0$ and $a/t = 0$. The upper curve was obtained from Lamé's stresses [10] on the inside of the cylinder and the solution for an edge-crack in a semi-infinite plate, and is given by eq. (5) with $a/t = 0$. The other curves show results from eq. (5) for various a/t ratios.

The stress-intensity factor for two symmetric surface cracks on the inside of a pressurized cylinder is given by eq. (3) where the following approximate expression for F has been fitted to the present results and those of references [8] and [9]:

$$F = 0.97 \left[M_1 + M_2 \left(\frac{a}{t} \right)^2 + M_3 \left(\frac{a}{t} \right)^3 \right] g f_\phi f_c \quad (6)$$

$$M_1 = 1.13 - 0.09 \frac{a}{c} \quad (7)$$

$$M_2 = 0.54 + \frac{0.89}{0.2 + \frac{a}{c}} \quad (8)$$

$$M_3 = 0.5 - \frac{1}{0.65 + \frac{a}{c}} + 14 \left(1 - \frac{a}{c} \right)^{24} \quad (9)$$

$$g = 1 + \left[0.1 + 0.35 \left(\frac{a}{t} \right)^2 \right] (1 - \sin \phi)^2 \quad (10)$$

$$\text{and } f_{\phi} = \left[\sin^2 \phi + \left(\frac{a}{c} \right)^2 \cos^2 \phi \right]^{1/4} \quad (11)$$

for $0 \leq \frac{a}{c} \leq 0.8$, $0 < \frac{a}{c} \leq 1$, $t/R \leq 0.25$, and any ϕ . Equation (6) is within about ± 5 percent of the finite-element results.

An estimate for the stress-intensity factors for a single crack in terms of two symmetric cracks was obtained from an equation (eq. (2)) given in reference [11]. For $a/c = 0$ and $t/R = 0.1$, the stress-intensity factor for a single crack was about 2 percent lower than that for two symmetric cracks, whereas for $t/R = 0.25$ the stress-intensity factor for a single crack was about 4 percent lower than that for two cracks. For larger a/c ratios the differences are smaller. Thus, eq. (6) can also be used for a single surface crack without appreciable error.

5.4 Comparisons with Other Solutions

Figure 6 shows the stress-intensity boundary-correction factors obtained by several investigators for a semi-elliptical surface crack ($a/c = 1/3$ and $a/t = 0.8$) on the inside of a cylindrical vessel with $t/R = 0.1$. The crack surfaces were subjected to stress distributions given by eq. (1). The correction factors, H_j , are those used in references [5] and [6], and are related to G_j by

$$H_j = \frac{B_j G_j}{f_{\phi}} \quad \text{for } j = 0 \text{ to } 3 \quad (12)$$

where $B_0 = 1$, $B_1 = \pi/2$, $B_2 = 2$, $B_3 = 3\pi/4$, and f_{ϕ} is given by eq. (11). The present results are shown as symbols. The results from reference [6], obtained from the boundary-integral equation method, are shown as solid curves and are in good agreement (± 2 percent) with the present results for $\phi > \pi/4$. The dashed curves show the results from reference [5]. Their results were obtained from the finite-element method and were within ± 8 percent of the present results. (For clarity, the results for H_2 were not shown.)

6. Concluding Remarks

A three-dimensional finite-element elastic stress analysis was used to calculate stress-intensity factors for a wide range of semi-elliptical surface cracks on the inside of cylindrical pressure vessels. The ratio of crack depth to crack length ranged from 0.2 to 1; the ratio of crack depth to wall thickness ranged from 0.2 to 0.8; and the ratio of wall thickness to vessel radius was 0.1 and 0.25. Singularity elements were used along the crack front and linear-strain elements were used elsewhere. The models of these configurations had about 6500 degrees of freedom. A nodal-force method was used to evaluate the stress-intensity factors.

The stress-intensity factors for surface cracks in pressurized cylinders were similar to those calculated for surface cracks in flat plates as a function of the parametric angle. For semi-circular cracks, the stress-intensity factors were maximum at the intersection of the crack with the inside surface of the cylinder, but for semi-elliptical cracks the values were largest at the maximum depth point. Larger crack-depth-to-wall-thickness ratios and larger wall-thickness-to-vessel-radius ratios gave higher stress-intensity factors for all surface-crack configurations considered.

The present results were compared to other analyses of internal surface cracks in cylinders. The surface-crack configuration had a crack-depth-to-wall-thickness ratio of 0.8, a crack-depth-to-crack-length ratio of 1/3, and a wall-thickness-to-vessel-radius ratio of 0.1. The cracks were subjected to constant, linear, quadratic, and cubic stress distribution on the crack surfaces. The results from a boundary-integral equation method were in good agreement (generally ± 2 percent) and those from a finite-element method were in fair agreement (± 8 percent) with the present results.

An empirical equation for the stress-intensity factors for an internal surface crack in a pressurized cylinder was developed to estimate the present results. The equation applies over a wide range of configuration parameters and was within about ± 5 percent of the present results. The results obtained herein should be useful in correlating fatigue-crack-growth rates and in calculating fracture toughness for the surface crack in a pressurized cylinder.

References

- [1] UNDERWOOD, J. H., "Stress Intensity Factors for Internally Pressurized Thick-Walled Cylinders," Stress Analysis and Growth of Cracks, ASTM STP-513, American Society for Testing and Materials, pp. 59-70 (1972).
- [2] KOBAYASHI, A. S., "A Simple Procedure for Estimating Stress Intensity Factors in Regions of High Stress Gradient," Significance of Defects in Welded Structures (T. Kanazawa and A. S. Kobayashi, eds.), University of Tokyo Press, pp. 127-143 (1974).
- [3] KOBAYASHI, A. S., EMERY, A. F., POLVANICH, N., and LOVE, W. J., "Inner and Outer Surface Cracks in Internally Pressurized Cylinders," J. Pressure Vessel Technology, ASME, pp. 83-89 (February 1977).
- [4] ATLURI, S. N., and KATHIRESAN, K., "Outer and Inner Surface Flaws in Thick-Walled Pressure Vessels," Transactions of the Fourth International Conference on Structural Mechanics in Reactor Technology, San Francisco, CA (1977).
- [5] MCGOWAN, J. J., and RAYMUND, M., "Stress Intensity Factor Solutions for Internal Longitudinal Semi-Elliptical Surface Flaws in a Cylinder under Arbitrary Loadings," 11th National Symposium on Fracture Mechanics, Blacksburg, VA (June 1978).
- [6] HELIOT, J., LABBENS, R. C., and PELLISSIER-TANON, A., "Semi-Elliptical Cracks in the Meridional Plane of a Cylinder Subjected to Stress Gradients," 11th National Symposium on Fracture Mechanics, Blacksburg, VA (June 1978).
- [7] RAJU, I. S., and NEWMAN, J. C., JR., "Three-Dimensional Finite-Element Analysis of Finite-Thickness Fracture Specimens," NASA TN D-8414 (1977).
- [8] RAJU, I. S., and NEWMAN, J. C., JR., "Improved Stress-Intensity Factors for Semi-Elliptical Surface Cracks in Finite-Thickness Plates," NASA TM X-72825 (1977).
- [9] RAJU, I. S., and NEWMAN, J. C., JR., "Stress-Intensity Factors for a Wide Range of Semi-Elliptical Surface Cracks in Finite-Thickness Plates," Engr. Fracture Mechanics 11, (4), pp. 817-829 (1979).
- [10] TIMOSHENKO, S., Strength of Materials, Advanced Theory and Problems, D. Van Nostrand Company, New York (1956).
- [11] SHAH, R. C., "Stress Intensity Factors for Through and Part-Through Cracks Originating at Fastener Holes," Mechanics of Crack Growth, ASTM STP-590, American Society for Testing and Materials, pp. 429-459 (1976).

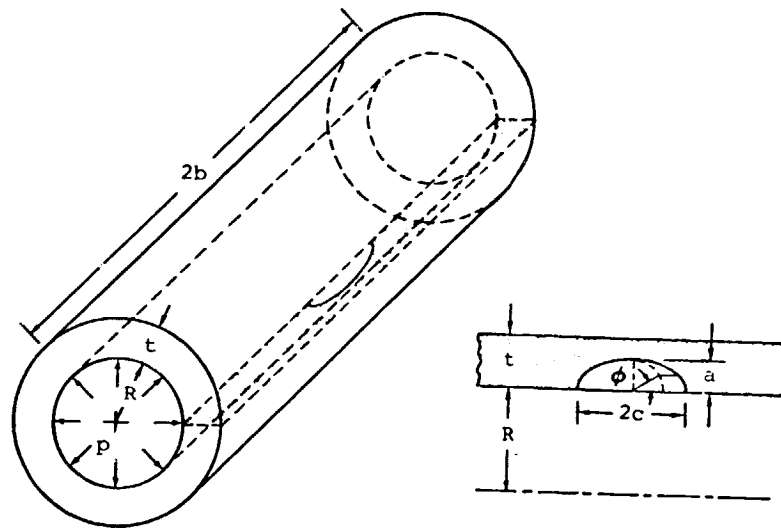


Fig. 1.- Surface crack in an internally pressurized cylinder.

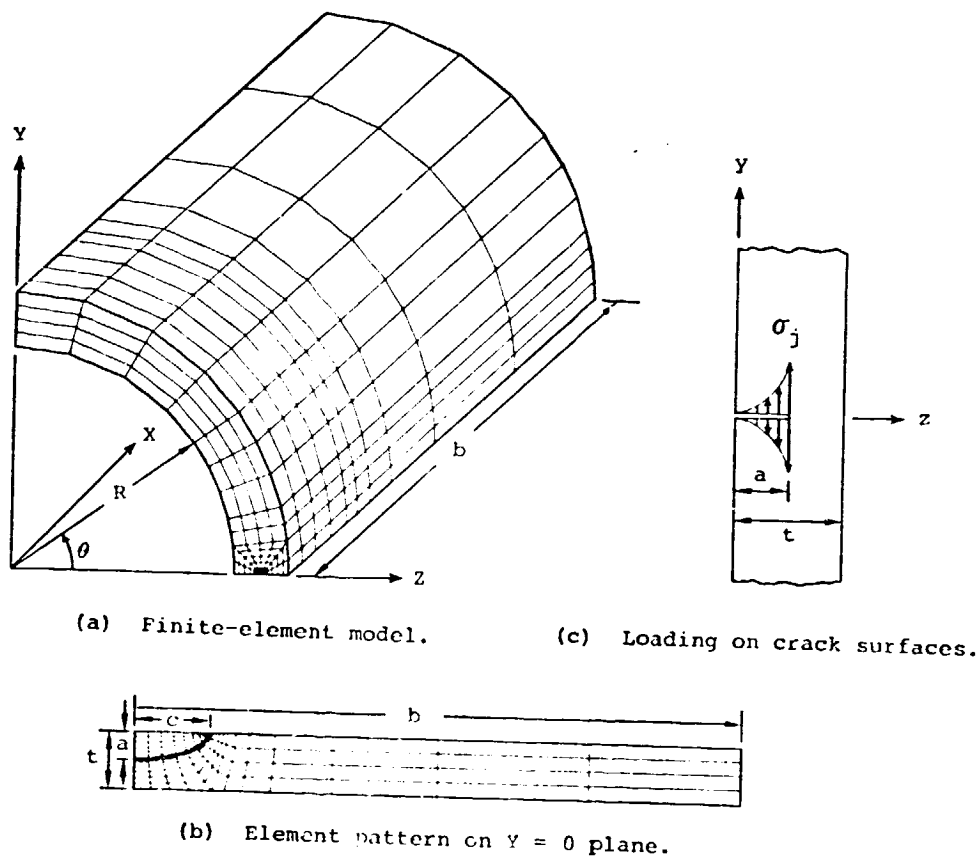


Fig. 2.- Finite-element model and loading on a semi-elliptical surface crack in a cylinder.

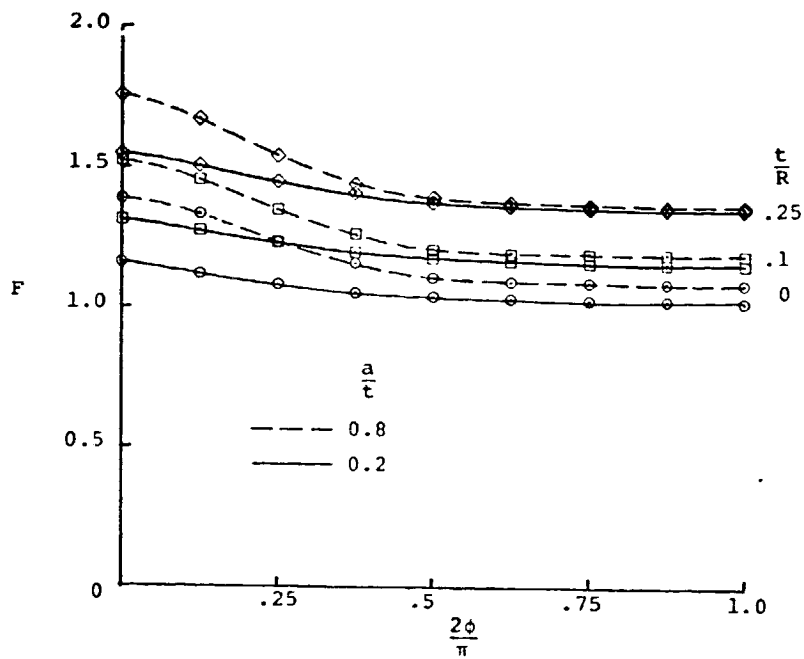


Fig. 3.- Stress-intensity boundary-correction factors along crack front for a semi-circular surface crack ($a/c = 1.0$) in a pressurized cylinder.

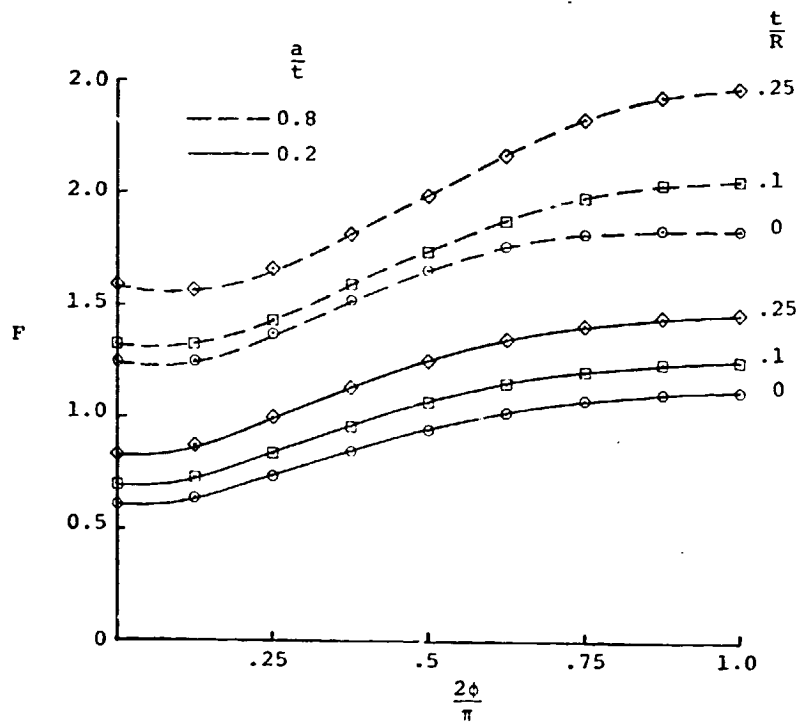


Fig. 4.- Stress-intensity boundary-correction factors along crack front for a semi-elliptical surface crack ($a/c = 0.2$) in a pressurized cylinder.

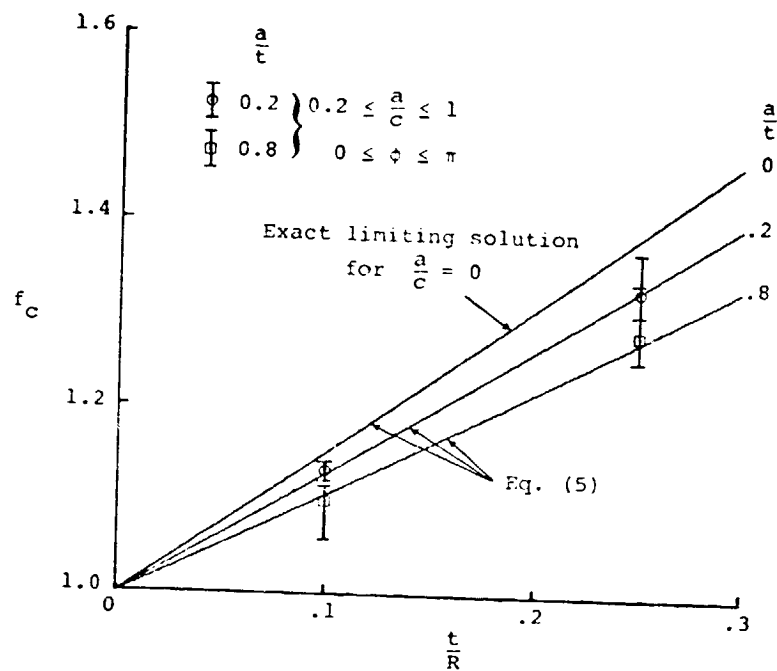


Fig. 5.- Boundary-correction factor for a surface crack in a pressurized cylinder normalized by the correction factor for a surface crack in a flat plate.

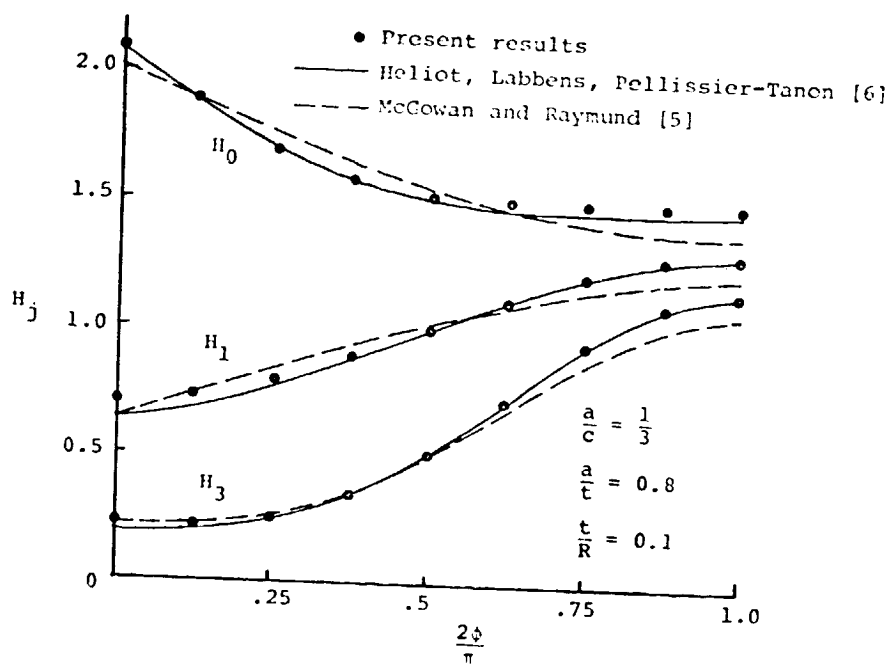


Fig. 6.- Stress-intensity correction factors computed by several methods for a semi-elliptical surface crack in a cylinder.

**END
DATE
FILMED**

SEP

12

1979